The revealing of regularities of the hydrocarbon combustion kinetics via the structure of a laminar flame front

Y. Kryzhanovskyi*

Research Centre "EcoEnergoComplex", Kiev, Ukraine

Abstract

This research of the laminar flame fronts of the premixed CH_4/air, C_3H_8/air and C_2H_2/air flames at various equivalence ratios was launched to reveal the general regularities of the kinetic mechanism of hydrocarbon combustion. The flame front thickness that is limited by the beginning and the end of chemical transformations, defined by the surfaces of minimal and maximal CO_2 concentrations coincides with the calculated by $\lambda_n = (D_{LP}^c/U_n)(T/T_0)^{1,5}$ and it is the chemical-physical constant of combustion. The H_2O concentration peaks within the flame fronts of CH_4/air, C_3H_8/air and C_2H_2/air flames correspond to the flame front thicknesses of H_2/air flames of the same H_2 specific concentrations. The radicals of the hydrocarbon combustion are formed at an independent burning-out of hydrogen with the simultaneous C-C bond breaking in accordance with their bond energies.

Introduction

Until now, only flame front propagation rate was considered as the basic constant of combustion. To explain the essential differences between laminar and turbulent combustion both laminar and turbulent propagation rates were used. But very many observations of the flame spreading processes require at least one more constant to be describable and to connect all dimensional characteristics of reaction wave. On the other side a volume reaction process needs one more constant connected to the reaction volume intensity.

Visibility of an ordered and a similar laminar flame front structure for the CH_4/air, C_3H_8/air and C_2H_2/air flames allowed us to draw a conclusion about the common kinetic mechanism of the consequent chemical reactions within a flame front existence. This work is dedicated to create a physically adequate concept of the normal flame front thickness as combustion constant as well.

Concept and calculation of the laminar flame front thickness

A normal flame front spreads with the flame propagation rate, U_n, and has the thickness, λ_n, can be characterized by an integral combustion constant, the specific volume intensity, that is given by:

$$\omega_{fr} = U_n / \lambda_n. \qquad (E1)$$

The value of $\boldsymbol{\lambda_n}$ represents the thickness of a plane reaction wave within that all the physical and chemical transformations of an initial mixture begin and finish.

Calculation method of the laminar flame front thickness is based on the next statements:

1. The thickness of a normal flame front is more in 10^6-10^7 than the free length of molecules and radicals. The number of reactions of the hydrocarbon combustion amounts to tens only therefore the flame front thickness and propagation rate are spotted by the molecular diffusion laws mostly.

2. For the $\boldsymbol{\lambda_n}$ estimation it is possible to assume that the formation beginning of the finish combustion products coincides with the forward boundary of a flame front and with the temperature increasing in it. The kinetic mechanism outruns the thermal conductivity in a gas mixture [1].

3. If several combustion products are formed within a flame front the limiting process product should be chosen. CO_2 is the limiting product (LP) of the combustion process for almost all hydrocarbons.

We state that the new CO_2 molecules formed in a front, originate reaction as a result of the first collisions after their formation when their temperature is close to the adiabatic combustion temperature, T_c [2].

From the previous statements and in accordance with the Fick's second low for the boundary conditions, $C_{LP} = C_{LP}^{max} (x/\lambda_n)$, the diffusion flow density, J, can be defined as:

$$J = D_{LP}^c (C_{LP}^{max}/\lambda_n). \qquad (E2)$$

As an average LP speed, W_{LP}, is equivalent to U_n [3, 15] and taking into account that $J = W_{LP} \cdot C_{LP}^{max}$ one may write:

$$\lambda_n = D_{LP}^c / U_n. \qquad (E3)$$

where D_{LP}^c – self-diffusion coefficient of the limiting reaction product at adiabatic combustion temperature.

If an initial temperature of a mixture, T, then the flame front thickness may be calculated by:

$$\lambda_n = (D_{LP}^c / U_n)(T/293)^{1,5}, \qquad (E4)$$

where U_n should be taken for the respective temperature of a mixture, and D_{LP}^c is determined as:

$$D_{LP}^c = D_0 \cdot (T^c/293)^n \cdot (1/P). \qquad (E5)$$

Depending on substance, n=1.8 – 1.95 [1]. For CO_2 and H_2O at standard conditions $D_{(0)}$ = 0.11 and 0.23 cm^2/s; n = 1.95 and 1.80 respectively [4].

Calculation results for the flame front thicknesses show a good conformity with the values measured by

* Corresponding author: ju.kryzhanovskiy@gmail.com

T-profiles and with the flame-spread critical spacings for different compounds and initial parameters.

Mixture	LP	U_n	D_0	P	T_c	λ_n (calc.)	λ_n (T-pr.)	$l_{cr(s)}$
-	-	cm/s	cm^2/s	bar	K	mm	mm	mm
CH_4/O_2	CO_2	330	0.11	1.0	3100	0.24		0.28
CH_4/O_2/Ar	CO_2	81	0.11	0.04	1850	13.4	14.0	-
30%H_2/air	H_2O	170	0.23	1.0	2260	0.62	0.64	0.62
20%H_2/air	H_2O	100	0.23	1.0	1910	0.69		0.70
10%H_2/air	H_2O	28	0.23	1.0	1440	1.48		1.50
7%H_2/air	H_2O	8	0.23	1.0	1000	2.67		2.80
$H_2/O_2/N_2$	H_2O	9	0.23	1.5	1076	3.42	3.50	-
H_2/O_2	H_2O	900	0.23	4.5	3020	0.12	0.13	-
21,8%NH_3-air	N_2	6	0.17	1.0	1750	7.80		7.80
19,0% NH_3-air	N_2	4	0.17	1.0	1460	8.50		8.60
17,0% NH_3-air	N_2	3	0.17	1.0	1260	9.88		10.0
NH_3/O_2	N_2	150	0.17	1.0	2400	0.62		0.65
$O_3 \rightarrow O_2$	O_2	54	0.18	1.0	1260	0.55	0.55	-
$N_2H_4 \rightarrow H_2$+ + NH_3 +N_2	N_2	155	0.17	1.0	1850	0.35	0.25	-

Table 1. Comparison of the λ_n calculated by (E4) with the measured by T-profiles and critical spacings.

The critical spacings, $l_{cr(s)}$, are taken from [5] for CH_4 /$2O_2$, CH_4/O_2/Ar, H_2/air flames, from [6] for NH_3/air, NH_3/O_2 flames. The λ_n defined by T-profiles are taken from [7] for CH_4/O_2/Ar flames, from [1] for H_2 /air flames, from [8] for $H_2/O_2/N_2$ flames, from [9] for $2H_2/O_2$ flames and decomposition reactions.

The analogous comparison for the different homologous series of hydrocarbons is presented below.

Mixture	Un, cm/s	T_c, K	λ_n, mm	$l_{cr(s)}$, absolutly min / stoich.
CH_4/air	31,0	2236	1.98	2,03 / 2,54
C_2H_6/air	35.5	2245	1.84	1.78 / 2.29
C_3H_8/air	34.5	2250	1.73	1.78 / 2.03
C_4H_{10}/air	33.5	2255	1.78	1.78 / 3.05
C_5H_{12}/air	34.0	2250	1.74	1.78 / 3.30
C_6H_{14}/air	34.0	2239	1.73	1.78 / 3.51
C_7H_{16}/air	34.0	2214	1.67	1.78 / 3.81
C_2H_4/air	62.0	2375	1.19	- / 1.27
C_3H_6/air	38.6	2339	1.64	- / 2.03
C_3H_6/air	42.0	2328	1.49	- / 1.78
C_6H_{12}/air	34.0	2250	1.74	1.78 / 3,06
C_6H_6/air	35.8	2305	1.72	1.78 / 2.79
C_2H_2/air	125.0	2700	0.71	- / 0.76
C_3H_6/air	62.5	2470	1.29	1.27 / 1.52

Table 2. Comparison of the λ_n calculated by (E4) at n=1.95, Φ=1.0 for the various homologous series of hydrocarbons with the flame-spread critical spacing [8].

Flame front concentration structure

The measuring carried out on the laminar flame front thickness at various equivalence ratios reveals the ordered concentration structure of a flame front, showed in Fig.1 [3]. We obtained the similar concentration structures for the flame fronts of CH_4/air, C_3H_8/air, 50%C_3H_8+50%C_4H_{10}/air and C_2H_2/air flames [3].

The results of experimental researches reveal three typical zones with new regularities for each zone: OA, AB, BC (Fig. 1) within a flame front.

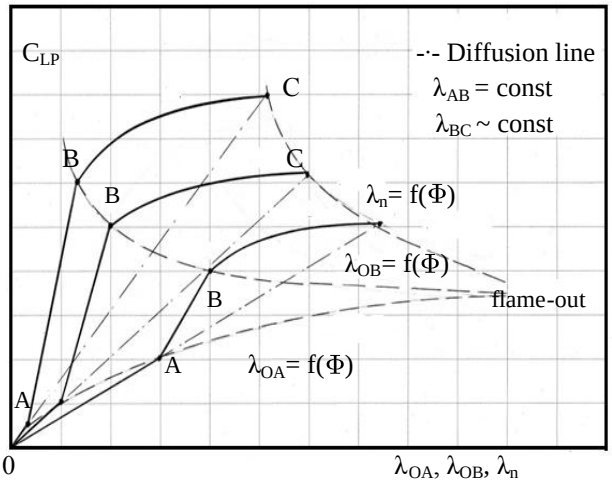

Figure 1. Structural diagram of a laminar flame front at various equivalence ratios and concentration limits

The points A for various Φ lie down on a convex curve, and the points B lie down on a concave curve. Both curves converge at the point related to the flame front thickness at a poor flame-out, and Φ corresponds to a lower concentration limit and at the same diffusivity (e.g. D≈2.2 cm^2/s for the CH_4/air flames).

Apparently the typical "break" of a CO_2-profile in a point A existence is the necessary requirement of a self-propagating reaction wave existence.

The plane laminar flame fronts were obtained on the round and slot burners with central stabilization.

Methane-Air Mixture (T_0= 293K)							
Φ	λ_{OA}	λ_{AB}	λ_{BC}	λ_n	T_A	T_B	T_C=T_c
1.08	0.34	0.2	1.41	2.05	540	725	2150
1.23	0.58	0.22	1.38	2.18	725	970	1625
1.45	1.03	0.2	1.39	2.59	920	1080	1440
1.70	2.20	0.2	1.32	4.02	1090	1080	1250
Propane-Air Mixture (T_0= 293K)							
Φ	λ_{OA}	λ_{AB}	λ_{BC}	λ_n	T_A	T_B	T_C=T_c
1.06	0.28	0.34	1.16	1.78	574	1130	2225
1.38	0.44	0.31	1.40	2.15	690	1120	1850
1.81	0.98	0.29	1.15	2.42	875	1120	1470
2.40	2.39	0.31	1.12	3.82	1024	1100	1260
λ are given in mm, T – in K.							

Table 3. Sizes of the typical zones of a flame front and temperature in points A, B and C.

The CO_2 formation reaction goes within OA segment by the mechanism that is essentially different

from the AB segment mechanism, where we observe a sharp increasing of CO_2 emission. The BC segment apparently doesn't have any special kinetic feature in comparison with AB. CO_2 emission decreasing is defined by the process of diffusion outlet there.

It's important to note that NO profile is similar to CO_2 profile along all three zones. This phenomenon needs a separate consideration and explanation.

To get an appropriate accuracy and verification of the measuring data we provided simultaneous measuring both concentration and temperature profiles. The last will coincide with the beginning and the end of chemical transformation if eliminate the radiation heat flux from a flame. The elimination method is described below.

T-profiles and the prove of the preheat zone absence

Assuming that the thermal conductivity, Λ, across a flame front is constant at a given density ρ_0 and heat capacity c_p then $\Delta T \sim \rho_0 \cdot c_p/\Lambda$. This complex is inverse to the thermal diffusivity, a. For the real gases $a = a_0 \cdot T^n$ if the exponent n is close to 2.0. Then T-profile within a flame front can be approximated by equation written as:

$$dT/dx = U_n (\rho_0 c_p/\Lambda) (T/T_0)^{-n}(T-T_0), \qquad (E6)$$

if integrate it at n = 1.9 – 1.95. Our measuring proved this approximation [2,3].

The next method allows us to eliminate the flame radiant flux effect on a thermocouple at approaching to a flame front and prove an absence of preheat zone before it. The temperature profiles built in relative co-ordinates $(T-T_0) / (T_c-T_0)$-x/λ_n at various equivalence ratios, extrapolate in a straight line that coincides with the chemical transformation beginning [2].

The thicknesses of CO_2 and temperature profiles are equal for the same mixtures. Thus, each of them can be used for the λ_n definition.

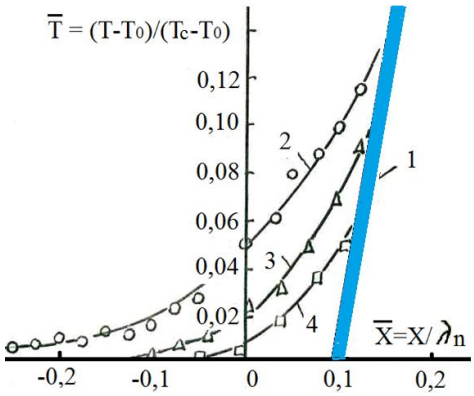

Figure 2. The flame radiation effect on the forward part of a T-profile at various Φ. 1 – The extrapolation line of the measured T profiles. 2, 3, 4- the measured profiles at Φ = 1.13; 1.29; 1.56 respectively.

An extrapolation line corresponds to the boundary of the chemical transformations beginning. So, we can conclude an absence of preheat zone before a flame front.

Measuring of H_2 concentration within a flame front

Measuring of H_2-profiles was conducted on the plane laminar flame front of a reverse flame that was obtained on the round and slot burners with central stabilization. The gas sampling was made by the microprobe of internal and external diameters 0.05mm and 0.15mm accordingly. The microprobe moving support resolution was 0.01mm. Displacement of front by a probe is no more than 0.1 mm while the front thickness is 2.1 – 4.5 mm.

Mixture	Φ	λ_{H2Omax}	λ_{OA}	λ_{CO2max}
	-	mm	mm	mm
CH_4/air	1.08	0.57	0.34	2.05
	1.23	0.72	0.58	2.18
	1.45	1.27	1.03	2.59
	1.70	1.90	2.20	4.02
C_3H_8/air	1.06	0.48	0.28	1.78
	1.38	0.54	0.44	2.15
	1.81	1.09	0.96	2.42
	2.40	2.34	2.39	3.82
C_2H_2/air	1.10	0.78		0.56
	2.06	1.12		0.81
	2.42	1.45		1.11
	3.05	3.25		2.82

Table 4. The measuring results of the H_2O and CO_2 concentration peaks within the flame fronts.

To provide the proper measurement accuracy we compared the concentration and temperature profiles that were measuring simultaneously by the platinum thermoelectric couple (Pt-Pt10%Rh) with a diameter of junction 0,05mm.

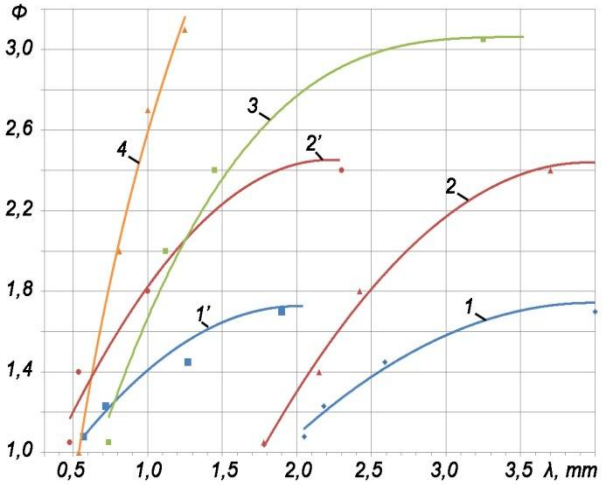

Figure 3. Comparison H_2O and CO_2 profiles for CH_4/air, C_3H_8/air, C_2H_2/air flames at various Φ. 1, 1'- CH4/air: $\lambda_n=\lambda_{CO2max}$ and λ_{H2Omax}; 2, 2' - C_3H_8/air: $\lambda_n=\lambda_{CO2max}$ and λ_{H2Omax}; 3 - C_2H_2/air: $\lambda_n=\lambda_{H2Omax}$; 4 - H_2/air: $\lambda_n=\lambda_{H2Omax}$.

For an additional improvement of measurement accuracy the following influencing factors have been considered by the method, described in [3]: the influence of the thermocouple junction diameter, influence of the flame front fluctuations with certain amplitude, radiation influence and temperature change of a sample microvolume.

Hypothesis about the H_2 burning-out mechanism

It is well known that in the gas-mixture/air flames the next sequence of burning-out takes place: hydrogen burns out at first, and then methane, and CO finally [10]. We assume that an analogous sequence remains for hydrocarbon combustion in spite of a bonded hydrogen.

In a flame front of CH_4/air flame at pressures 0.5, 0.1 and 0.05 bar H_2O-profiles coincide if their coordinates increase or divide two times [11]. We assume that the observed coincidence is a special case of a common property of all concentration profiles, defined by the combustion kinetics.

The bond breaking energy of H-atom in molecules and radicals, Δh_H^*, is a rather close to the bond energy of H-H, especially for the paraffin hydrocarbons. Therefore, hydrogen bonded to carbon, is practically equivalent to molecular hydrogen at conbustion.

Compound	Δh_H^*, kcal/mole	Compound	Δh_H^*, kcal/mole
H – H	103,3	iso – C_3H_7 – H	94
CH_3 – H	103	n – C_4H_9 – H	94
C_2H_5 – H	98	C – H	81
n-C_3H_7– H	95	(CH_2=CH_2)–H	104

Table 5. The bond energies of H-atom in some molecules and radicals [3, 14].

On the base of the presented above, we suppose hydrogen consisted in hydrocarbons burns-out as if it is in a free molecular state.

From Table 2 we can conclude the very different hydrocarbons have the almost same flame front thicknesses and the critical flame-spread spacings. Therefore, the mechanism of chemical transformations apparently goes on in accordance with the algorithm inclusive two next stages:

1. Decomposition of C-C, C=C and C≡C bonds.
2. The hydrogen burning-out if it is in a free molecular state.

Let's verify the proposed mechanism of the hydrogen burning-out on the methane/air flames to avoid an additional influence of C-C bonds. The equation for the thicknesses of the maximum H_2O concentration reaching, $\lambda_{(H2O)}$, can be obtained on the base of the next assumption.

Hydrocarbons make an inhibiting impact on H_2 burning. It is revealed, for example, in a diversion from the Le Chatelier Principle for the flame spread limits of a hydrogen-air flame with small additives of CH_4, CH_3OH and other hydrocarbons [12]. It's natural to assume that the same inhibiting influence exists even at burning hydrogen consisted in hydrocarbons.

So $\lambda_{n(CH4)}$ is spotted by diffusion rate of the LP - CO_2. At the same time hydrogen burns-out as assumed with the flame propagation rate of the H_2/air mixture with the same H_2 volume concentration. Or the other hand, the value of $\lambda_{n(H2)}$ for the CH_4/air flame front should be decreased in accordance with the $U_{n(CH4)}/U_{n(H2)}$ ratio in order to correspond to that propagation rate and can be determined as:

$$\lambda_{(H2O)} = (U_{n(CH4)}/ U_{n(H2)})\cdot \lambda_{n(CH4)}, \qquad (E7)$$

where $U_{n(H2)}$ should be taken for the mixture of the same H_2 concentration as a given mixture; D^c_{CO2} should be taken at a combustion temperature of a given mixture. Using (E3) one may write:

$$\lambda_{(H2O)} = D^c_{CO2}/ U_{n(H2)}. \qquad (E8)$$

Φ	$U_{n(CH4)}$	H_2	$U_{n(H2)}$	λ_n	$\lambda_{(H2O)}$ calcul.	$\lambda_{(H2O)}$ profile
-	cm/s	%	cm/s	mm	mm	mm
1.05	30	15.9	95	2.01	0.63	0.59
1.20	23	13.8	65	2.15	0.76	0.71
1.50	13	11.6	30	2.93	1.27	1.30
1.70	7.5	10.2	20	4.02	1.51	1.90
1.90	3.5	9.4	12	7.85	2.29	2.38

Table 6. The comparison of $\lambda_{(H2O)}$ calculated by (E8) with the experimental data from Table 4 and Figure 3.

The calculation results for propane/air, propane /butane/air flames give an analogous conformity. For all tested compounds and flames at various Φ we received: $\lambda_{(H2O)} = (0.3 - 0.5)\cdot\lambda_n$.

These calculations confirm the hypothesis about the hydrogen burning-out mechanism for all hydrocarbons besides acetylene. The parameters of the acetylene combustion needs a separate discussion, we consider this case in detail below.

Chemical interpretation of the flame front structure

Thickness of OA zone increases promptly together with Φ increasing and OA line remains as a part of a diffusion straight line, $C_{LP} = C_{LP}^{max}\cdot(x/\lambda_n)$. Thickness of AB zones is constant at given T_0 and does not depend on Φ (Table 2).

The H_2O concentration peak matches a rare part of OA segment or an initial part of AB segment. The comparison of H_2O and CO_2 concentration profiles of the CH_4/air flame fronts give possibility to assume that the CO_2 formation within OA segment doesn't occur as a branching chain reaction, but it is defined by the hydrogen burning-out.

For methane combustion the CO_2 formation chain can be determined as [13]:

$$CH_4 \rightarrow CH_3 \rightarrow CH_2O \rightarrow CHO \rightarrow CO. \qquad (R1)$$

Let's consider how the molecular structure affects the combustion kinetic mechanism.

The combustion constants are the integral characteristics of the chemical kinetics and the regularities revealed before, allows to make an assumption and about the kinetic order of chemical transformations at the hydrocarbon combustion.

The influence of C-C bond existence on the combustion kinetics will be deliberately examined below.

The bond energy of hydrogen atom in the CH_2-group of the paraffin hydrocarbons does not change practically from the fifth carbon atom from the chain ends [14].

93,6-88,8-86,9-86,1-85,8-85,7-85,7-85,8-86,1-86,9-88,8- 93,6
C - C - C - C - C - C - C - C - C - C - C - C - C

Figure.4. The bond energies of H atom in CH_2-group of the paraffin hydrocarbons, (kcal/mole).

The C-C bond energy is less than C-H bond energy. The CH_3-CH_2 bond breaking energy is more than the CH_2-CH_2- bond breaking energy. Some values of the bond breaking energies are given below:

CH_3–CH_3 …….86.0	C_2H_5–C_2H_5…….....79,5
C_2H_5–CH_3 ……80.5	n-C_3H_7–C_3H_7 ……76,0
C_3H_7–CH_3…….81.0	n–C_4H_9–CH_3 ……80,0

Table 7. The bond breaking energies for some hydrocarbon groups, (kcal/mole).

Just the ratios of the bond breaking energies (e.g. in accordance with Fig.4) define the sequence of the long-chain molecules breaking in a flame front of hydrocarbons.

The beginning of the methane combustion defined rather good [13]:

$$CH_4 + M \rightarrow CH_3 + H + M. \qquad (R2)$$

The role of M particle accomplishes H, OH, O, etc. In accordance with Fig. 4, it is much more probable that hydrogen breaks from the middle of a chain by the mechanism, analogous to (R2).

Therefore, in accordance with our kinetic model for the propane combustion we can write:

$$C_3H_8 \rightarrow CH_2O+CH_2O+CH_2O \rightarrow CHO \rightarrow CO. \quad (R3)$$

The rather different values of U_n and the changing of LP to H_2O for C_2H_2/air flames apparently correspond to the kinetic mechanism when the C≡C bond breaking and the hydrogen burning-out happen simultaneously. Thus, for the acetylene combustion the next reaction takes place:

$$C_2H_2 \rightarrow CHO + CHO \rightarrow CO. \qquad (R4)$$

For acetylene the CO_2 formation chain is much shorter than for methane and this mechanism outruns the H_2O formation or their rates are very close one to the other. The flame front thickness for acetylene is apparently determined by the H_2O concentration maximum and by the thickness of H_2O profile. Taking H_2O as the LP for C_2H_2/air flame we get λ_n = 0.93mm and taking CO_2 as the LP we will get λ_n = 0.71mm (Tab.2). Our experimental data give λ_n about 0.8mm. May be in case of acetylene the breaking bonds process and the H_2 burning-out processes happen simultaneously. For comparison the flame front thickness of hydrogen at Φ=1.0 is about 0.6mm.

Thus, we can consider that the intermediate compounds and radicals are formed not as a result of a consecutive chain reaction, but arise at an independent "burning-out" of hydrogen along with the simultaneous C-C bond breaking with the sequence spotted by their bond energies.

The fact that for the λ_n of the C_6H_{14}/air and C_7H_{16}/air flames is less than for CH_4/air flames proves this statement.

Using the approach described above, we can explain that the very similar hydrocarbons cannot be united by the common U_n description. The empirical coefficients entered in this description, reflect properties of a very small group of the hydrocarbon compounds. Even the hydrocarbons from the same homologous series with the same molecular weight and an almost equal adiabatic combustion temperature can differ in propagation rate considerably. For example, 1-butin and 2-butin have T_c 2413K and 2401K respectively, U_n = 58.1 cm/s and 51.5 cm/s respectively. The structure difference C≡C-C-C, and C-C≡C-C respectively changes a kinetic process essentially and in accordance with our reasoning their combustion process goes on via different radicals. It leads to the different empirical coefficients entered into relations for U_n [4]. If analyze Table 2 we can note that the C=C and C≡C bonds existence in some hydrocarbons leads to the U_n and T_c increasing and to the λ_n decreasing.

Conclusions

1. The laminar flame front thickness is the second basic constant of combustion and together with the propagation rate of a flame front determines the specific volume intensity of a flame front and the specific volume intensity of any flame independently on its turbulence level.

2. A laminar flame front has an ordered concentration structure of three typical zones with the different regularities defined by diffusion lows. The preheat zone before a flame front is absent.

3. Hydrogen consisted in hydrocarbons burns-out as if it is in a free molecular state.

4. The intermediate compounds are formed within a flame front as a result of an independent burning-out of hydrogen and the C-C bond breaking with the sequence spotted by their bond energies.

References

[1] V. Kryzhanovsky, Recent Developments in the Theory of combustion of Gases, HTR, v. 24, №4, USA, (1992).

[2] V. Kryzhanovsky, Y. Kryzhanovsky, A scientific controversy in combustion theory, Osvita Ukrainy, Kiev, Ukraine (2011) p. 175.

[3] V. Kryzhanovsky, *Phenomenological bases of combustion theory of gases*, PhD Thesis, Academy of science ICP, Chernogolovka, USSR, 1986.

[4] P. Atkins, Physical chemistry, 5th ed. Freeman, New York, USA (1996).

[5] R. Fristrom, Flame structure and processes, Oxford University Press, New York/Oxford, USA (1995).

[6] C. Vagelopoulos, F. Egolfopoulos, Direct experimental determination of laminar flame speeds. Proc. Comb. Inst. 27:513 (1998)

[7] P. Stephenson, R. Taylor, Combust. Flame 20 (2) (1973) 231–244.

[8(53)] F. Williams, Combustion theory, Benjamin/ Cummings, Menlo Park, CA (1985) p. 704.

[9] J. Longwell, Speed of high-temperature reactions at burning of hydrocarbons, VRT, USA (1956).

[10] M. Fox, F. Weinberg, 13-th Symp. on Combust., Pittsburgh, Pensylvania (1971) 641–648.

[11] R. Fristrom, A. Westenberg, Flame Structure, McGraw-Hill, USA (1965) p. 424.

[12] C. Bertrand, R. Delbourgo, Combust. Flame, 41 (3) (1981)235–242.

[13] G. Aravin, E. Semenov, Interconnection between the ionization and reaction rates in a laminar flame, Academy of science ICP, v. 15, №5, USSR, (1979) 40-46.

[14] N. Suzuki, V. Oba, T. Hizano, Bull. JSME, v. 22, (1979) 848-856.

[15] Y. Kryzhanovskyi, The Internal Structure of a Flame Front and Combustion Constants, Proc. ECM 2013.